INVESTIGATION ON THE DRAG COEFFICIENT OF SUPERCRITICAL WATER FLOW PAST SPHERE-PARTICLE AT LOW REYNOLDS NUMBERS

by

Zhenqun WU, Hui JIN*, and Leijin GUO

State Key Laboratory of Multiphase Flow in Power Engineering,
Xi'an Jiaotong University, Xi'an, Shaanxi, China

Original scientific paper
https://doi.org/10.2298/TSCI17S1217W

Supercritical water fluidized bed is novel reactor for the efficient gasification of coal to produce hydrogen. The Euler-Euler and Euler-Lagrange methods can be used to simulate the flow behaviors supercritical water fluidized bed. The accuracy of the simulated results with the two methods has a great dependence on the drag coefficient model, and there is little work focused on the study on particle's drag force in supercritical water. In this work, the drag coefficients of supercritical water flow past a single particle and particle cluster. The simulated results show that the flow field and drag coefficient of single particle at supercritical condition have no difference to that at ambient conditions when the Reynolds number is same. For the two-particles model, a simplification of particle cluster, the drag coefficients of the two particles are identical at different conditions for the same Reynolds number. The variation characteristics with the Reynolds number and particles' positions are also same.

Key words: *drag coefficient, supercritical water, single particle, particle cluster*

Introduction

In recent years, the supercritical water fluidized bed (SCWFB) has been a novel reactor for the efficient gasification of coal to produce hydrogen [1-4]. Constrained by the high pressure and temperature, the experimental detail investigation is difficult to carry out [5, 6]. Numerical simulated technology provides a convenient access to the insight of the flow behaviors inside the SCWFB and the Euler-Euler method and Euler-Lagrange method have been widely applied to granular flow simulation [7]. The accuracy of these methods has a great dependence on the drag force model, which is a necessary term for describing the momentum transfer between the solid and fluid phase.

The flow of viscous fluid past a stationary isolated sphere is considered as a simplified and fundamental case for the study of the particle's drag coefficient. Rouse [8] gave a graphical presentation of drag coefficient as a function of Reynolds number, which derived from experimental data. The drag coefficient was also expressed in an analytical form and some empirical expressions can present acceptable results for a wide Reynolds number range [9-11]. The drag force of particle cluster in the multiphase system has been also studied by many researchers through experimental method. Many semi-empirical correlations have been reported in litera-

* Corresponding author, e-mail: jinhui@mail.xjtu.edu.cn

ture, such as the Ergun model [12], Wen *et al.* model [13], Gidaspow model [14], and so on. These models have been widely used in the simulation of particle-fluid system.

However, most of the drag coefficient models are derived from the regression of the experiment and numerical simulated data in ambient condition, and there has been little attention focused on the study of the supercritical water (SCW) flow past sphere particle. As the unique physical property of SCW, this work was aimed to study the flow field and drag coefficient of SCW flow past sphere-particle and validate the application of the existing drag coefficient models.

Numerical formulation

In this work, the SCW flowed past the sphere-particle for Reynolds number of 10 to 200. So, a laminar incompressible steady flow model was used:

$$\nabla\vec{\mathrm{u}} = 0 \tag{1}$$

$$\frac{\partial}{\partial t}\vec{\mathrm{u}} + (\vec{\mathrm{u}}\nabla)\vec{\mathrm{u}} = -\frac{1}{\rho}\nabla p + \mu\nabla^2\vec{\mathrm{u}} \tag{2}$$

where $\vec{\mathrm{u}}$ is the velocity, ρ – the density, p – the pressure, μ – the viscosity, and t – the time. The drag force and drag coefficient can be calculated:

$$F_{\mathrm{d}} = \mu\int_s \vec{\mathrm{u}}\vec{\mathrm{n}}\mathrm{d}S + \int_s p\vec{\mathrm{i}}\vec{\mathrm{n}}\mathrm{d}S \tag{3}$$

$$C_{\mathrm{d}} = \frac{F_d}{\frac{1}{2}\rho u^2\frac{1}{4}\pi D^2} \tag{4}$$

where $\vec{\mathrm{n}}$ is the unit normal vector of surface, and $\vec{\mathrm{i}}$ is the unit vector in the X-direction.

Numerical consideration

As the axisymmetric characteristic of the flow regime, a quarter of the simulated domain was taken into adoption. The schematic diagram of the simulated domain was shown in fig. 1. To avoid the boundary blockage effect, the size of the flow domain was chosen as $40D \times 20D \times 20D$ corresponded to the X-, Y-, and Z-directions. The D is the particle diameter with the value of 0.0002 m. The particle was located in the center of the Y- and Z-direction and $10D$ to the left patch. In fig.1, the left and right patches were set as inflow and outflow, respectively. The front and bottom patches were both set as symmetrical boundary. The top and back

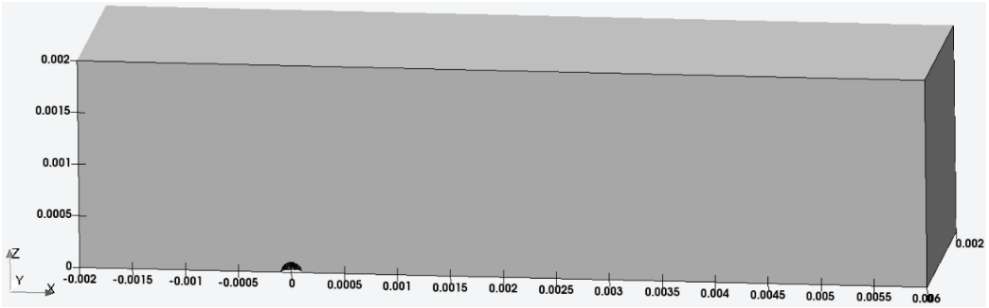

Figure 1. Schematic diagram of the flow domain

patches were set as slid boundary. The surface of the particle was set as no-slip boundary. In this work, as the heat transfer was not taken into account, the properties of the water with certain temperature and pressure was calculated based on the IAPWS-IF97 equations and kept constant during the flow process.

The flow domain was discreted into meshes through SnappyHexMesh, one mesh generation utility of OpenFOAM. In this method, the mesh density was controlled by the size of the background mesh size and the refinement level of the geometry surface. For the mesh independence validation, two kinds of uniform cubic background mesh size, $2e^{-5}$ m and $1.33e^{-5}$ mm, and three kinds of refinement level, 3, 4, 5, were taken into account. When the Reynolds number of inflow was 100 and the simulated condition was 0.1 MPa and 300 K , the simulated results were shown in tab. 1.

From tab. 1, it can be seen that the background mesh with the size of $1.33e^{-5}$ m and the refinement level of 4 is fine enough for the simulation.

Table 1. Results of mesh independence validation

Mesh size	$2e^{-5}$ m	$2e^{-5}$ m	$1.33e^{-5}$ m	$1.33e^{-5}$ m	$1.33e^{-5}$ m
Level	3	4	3	4	5
Mesh number	161740	212798	502211	614959	1057989
C_D	1.138	1.116	1.104	1.089	1.088

Simulated results

Numerical method validation

To validate the accuracy of the numerical method, the water flow past a single particle at ambient condition (0.1 MPa and 300 K) was simulated firstly. The simulated results of the drag coefficient were compared to the calculated results based on the empirical equations published in [9, 15-17]. The comparison was shown in fig. 2. In the figure, it can be seen that the simulated results have the best consistence with the calculated results based on Clift model. When the Reynolds number is 10, there is the maximum deviation between all the results and the deviation between the results of simulation and the Clift model is 1.28%. So, the accuracy and reliability of numerical method was validated.

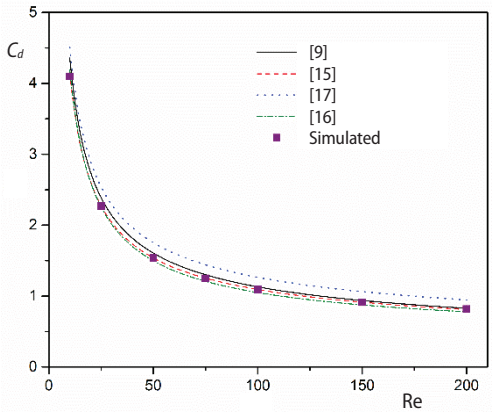

Figure 2. Comparison of simulated drag coefficient to that calculated by empirical equations

The SCW water flow past a single particle

In the supercritical condition, the water becomes a fluid medium which different from both the liquid and gas. Especially near the critical point, the properties of water change dramatically. Table 2 shows the simulated drag coefficients of water flow past a single particle for different Reynolds number at the pressure 23 MPa, and the temperatures 633.15-693.15 K, 773.15 K, and 873.15 K. The results were compared to those at 300 K and 0.1 MPa. From the table, it can be observed that there is little difference for the same Reynolds number at the different operating conditions.

Table 2. Drag coefficient at different conditions

Re	10	25	50	75	100	150	200
23 MPa, 633.15 K	4.0981	2.2705	1.5372	1.2496	1.0890	0.9114	0.8158
23 MPa, 643.15 K	4.0982	2.2710	1.5372	1.2496	1.0890	0.9114	0.8158
23 MPa, 653.15 K	4.0981	2.2723	1.5375	1.2496	1.0891	0.9115	0.8158
23 MPa, 663.15 K	4.0981	2.2725	1.5374	1.2497	1.0890	0.9115	0.8158
23 MPa, 673.15 K	4.0983	2.2716	1.5374	1.2496	1.0891	0.9115	0.8158
23 MPa, 683.15 K	4.0981	2.2711	1.5374	1.2496	1.0886	0.9115	0.8158
23 MPa, 693.15 K	4.0982	2.2707	1.5372	1.2496	1.0890	0.9115	0.8158
23 MPa, 773.15 K	4.0968	2.2695	1.5371	1.2495	1.0890	0.9115	0.8158
23 MPa, 873.15 K	4.0980	2.2688	1.5370	1.2495	1.0890	0.9115	0.8158
0.1 MPa, 300 K	4.0978	2.2713	1.5370	1.2495	1.0890	0.9114	0.8157

Figure 3 illustrates the streamlines around the particle at the pressure 0.1 MPa and the temperatures 300 K , 23 MPa, and 773.15 K for the Reynolds number of 25, 50, 100, and 200. As can be seen in the figure, the flow field at two different conditions is in good consistence. For the Reynolds number of up to 200, the simulated results at the supercritical condition present steady axisymmetric flow, which comparing well with the published numerical and experimental data at ambient conditions [18].

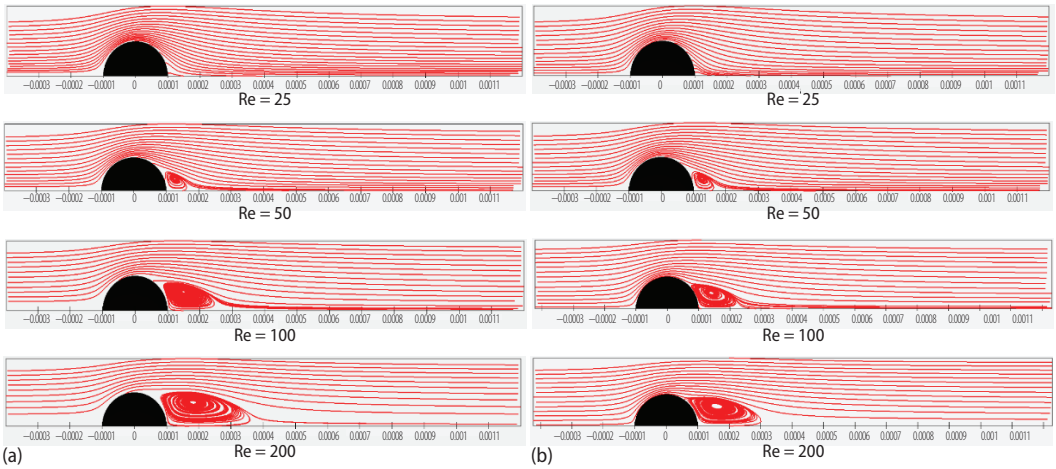

Figure 3. Streamline around the particle: (a) series at 0.1 MPa and 300 K , and (b) series at 23 MPa and 773.15 K

Conclusions can be obtained that for the same Reynolds number 200, the hydrodynamics of the water flow past at the supercritical condition is same with that at the ambient condition and the empirical equations for calculating the drag coefficient of single particle can be also applied in supercritical conditions.

The SCW flow past two particles

The drag coefficient of particle cluster is much more complicated than that of single particle as the particles' direct interaction and the influence of the surrounded particles through the flow field. In the general simulated study of particle-fluid multiphase system, the particles' interaction is referred to the particles collision, which is depended on the set of the particle's

properties. As a result, for the study of the drag coefficients of the SCW flow past particle cluster, we focused on the influence of the surrounded particles to the flow field. For simplification, a two-particle model was used to study the influence each other. The flow domain and the mesh density for single particle were also used in this part. In the two-particle model, two particles were distributed in the line of inflow direction, where the particle has the most influence on the each other through the flow field. The front particle was defined as P1, and the other one was P2. The distance between two particles was referred to as L. Tables 3, 4, and 5 show the drag coefficient of the two particles for different Reynolds numbers at the pressures 0.1 MPa and the temperatures 300 K, 23 MPa, and 633.15 K, 23 MPa and 773.15 K, and 23 MPa, when L/D is 1, 2, 3.

From the tables, it can be seen that the drag coefficients of the two particles decrease comparing to that of single particle as the influence of each other, especially for P2. With the increase of Reynolds number, the influence on P1's drag coefficient become weaken, but it is opposite for P2. This is because of that P2 located at the rear wake zone of P1, the fluid velocity around P2 is small, and P2 reinforce the influence of the recirculation on P1. When Reynolds number increases, the enlarged rear wake zone of P1 results in the fluid velocity around P2 becoming smaller and the influence of P2 on the recirculation getting more reinforcement. It can be also observed that, with the value of L/D increasing, the influence of the two particles between each other get weaken. By comparing the results at different conditions, it can be ob-

Table 3. Drag coefficients for two particles when $L/D = 1$

Re		10	25	50	75	100	150	200
0.1 MPa, 300 K	P1	3.4302	1.9819	1.3771	1.1368	1.0041	0.8599	0.7839
	P2	1.9795	0.9284	0.5250	0.3674	0.2769	0.1691	0.1039
23 MPa, 633.15 K	P1	3.4303	1.9835	1.3772	1.1371	1.0041	0.8599	0.7840
	P2	1.9806	0.9290	0.5249	0.3672	0.2767	0.1687	0.1039
23 MPa, 773.15 K	P1	3.4304	1.9834	1.3772	1.1371	1.0041	0.8599	0.7838
	P2	1.9805	0.9290	0.5250	0.3674	0.2769	0.1684	0.1031

Table 4. Drag coefficients for two particles when $L/D = 2$

Re		10	25	50	75	100	150	200
0.1 MPa, 300 K	P1	3.7396	2.1003	1.4242	1.1576	1.0100	0.8513	0.7693
	P2	2.4397	1.1991	0.7151	0.5255	0.4163	0.2892	0.2149
23 MPa, 633.15 K	P1	3.7400	2.0998	1.4243	1.1576	1.0100	0.8513	0.7693
	P2	2.4400	1.1987	0.7151	0.5253	0.4162	0.2891	0.2147
23 MPa, 773.15 K	P1	3.4304	2.0999	1.4243	1.1576	1.0100	0.8514	0.7694
	P2	2.4398	1.1987	0.7150	0.5252	0.4161	0.2889	0.2141

Table 5. Drag coefficients for two particles when $L/D = 3$

Re		10	25	50	75	100	150	200
0.1 MPa, 300 K	P1	3.9124	2.1870	1.4807	1.2007	1.0427	0.8662	0.7716
	P2	2.7579	1.3826	0.8447	0.6373	0.5213	0.3918	0.3215
23 MPa, 633.15 K	P1	3.9128	2.1866	1.4808	1.2007	1.0428	0.8662	0.7716
	P2	2.7582	1.3822	0.8447	0.6372	0.5213	0.3918	0.3215
23 MPa, 773.15 K	P1	3.4304	2.1866	1.4809	1.2007	1.0427	0.8662	0.7717
	P2	2.7582	1.3822	0.8447	0.6372	0.5213	0.3918	0.3213

served that, the drag coefficients of the two particles at different conditions have no difference when the Reynolds number is same. The variation characteristics with Reynolds number and the value of L/D are identical, which imply that the inter-particle influence through the flow field are same at the ambient and supercritical conditions.

So, it can be also concluded that the empirical equations for calculating the drag coefficient of particle cluster are applicable at supercritical conditions.

Conclusions

In this work, it was numerically studied that the drag coefficient of the SCW flow past single particle and particle clusterat low Reynolds numbers. A laminar incompressible steady flow model was adopted. From the simulated results, conclusions can be generated as follow.

- For a single particle, the drag coefficient and flow field are same for the same Reynolds number and there is no differcence between different conditons.
- The emperical equations for calculating the drage cofficient of the single particle can be also applicable at supercritical condition.
- For the two-particle model, a simplification of the particle cluster, the drag coefficients of the two particles have the same value, and the inter-particle influence through the flow field is same at the ambient and supercritical conditions.
- The empirical equations for calculating the drag coefficients of the particle cluster can be also applicable at the supercritical conditions.

Acknowledgment

This work was financially supported by the National Key R&D Program of China (Contract No.2016YFB0600100), and the National Natural Science Foundation of China (Contract No. 51323011 and 51776169).

Nomenclature

C – drag coefficient
D – particle diameter, [m]
d – drag, [–]
F_d – drag force, [N]
$\vec{\mathrm{i}}$ – unit vector in X-direction, [–]
$\vec{\mathrm{n}}$ – unit normal vector of surface, [–]
p – pressure, [Pa]
Re – Reynolds number (= $\rho uD/\mu$)
S – surface area, [m^2]
t – time, [s]
u – module of velocity, [ms^{-1}]
$\vec{\mathrm{u}}$ – velocity, [ms^{-1}]

Greek symbols

ρ – density, [kgm^{-3}]
μ – viscosity, [m^{2}s^{-1}]

Acronyms

SCW – supercritical water
SCWFB – supercritical water fluidized bed

References

[1] Cao, C., *et al.*, System Analysis of Pulping Process Coupled with Supercritical Water Gasification of Black Liquor for Combined Hydrogen, Heat and Power Production, *Energy, 132* (2017), 1, pp. 238-247
[2] Jin, H., *et al*., Supercritical Water Synthesis of Bimetallic Catalyst and Its Application in Hydrogen Production by Furfural Gasification in Supercritical Water, *International Journal of Hydrogen Energy, 42* (2017), 8, pp. 4943-4950
[3] Cao, W., *et al*., Hydrogen Production from Supercritical Water Gasification of Chicken Manure, *International Journal of Hydrogen Energy, 41* (2017), 48, pp. 22722-22731
[4] Jin, H., *et al*., Experimental Study on Hydrogen Production by Lignite Gasification in Supercritical Water Fluidized Bed Reactor Using External Recycle of Liquid Residual, *Energy Conversion and Management, 145* (2017), 1, pp. 214-219

[5] Lu, Y., *et al.*, A Numerical Study of Bed Expansion in Supercritical Water Fluidized Bed with a Non-Spherical Particle Drag Model, *Chemical Engineering Research and Design*, *104* (2015), Dec., pp. 164-173
[6] Jin, H., *et al*., Experimental Investigation on Methanation Reaction Based on Coal Gasification in Supercritical Water, *International Journal of Hydrogen Energy, 42* (2017), 7, pp. 4636-4641
[7] Sinclair, J. L., *Multiphase Flow and Fluidization: Continuum and Kinetic Theory Descriptions: By Dimitri Gidaspow*, Academic Press, New York, USA, 1994
[8] Rouse, H., *Nomogram for the Settling Velocity of Spheres*, National Research Council, Washington DC, USA, 1938
[9] Turton, R., Levenspiel, O., A Short Note on the Drag Correlation for Spheres, *Powder Technology*, *47* (1986), 1, pp. 83-86
[10] Flemmer, R. L. C., *et al.*, On the Drag Coefficient of a Sphere, *Powder Technology*, *48* (1986), 3, pp. 217-221
[11] Almedeij, J., Drag Coefficient of Flow Around a Sphere: Matching Asymptotically the Wide Trend, *Powder Technology*, *186* (2008), 3, pp. 218-223
[12] Ergun, S., Fluid Flow Through Packed Columns, *Chem.eng.prog*, *48* (1952), 2, pp. 89-94
[13] Wen, C., *et al.*, Mechanics of Fluidization, *Proc. Chem. Eng. Prog. Symp. Ser.*, *62* (1966), pp. 100-111
[14] Gidaspow, D., *Multiphase Flow and Fluidization: Continuum and Kinetic Theory Descriptions*, Academic Press, New York, San Diego, Cal., USA, 1994
[15] Clift, R., *et al.*, *Bubbles, Drops, and Particles*, Academic Press, New York, USA, 1978
[16] Khan, A. R., Richardson, J. F., The Resistance to Motion of a Solid Sphere in a Fluid, *Chemical Engineering Communications*, *62* (1987), 1-6, pp. 135-150
[17] Schiller, L., Naumann, A. Z., Uber Die Grundlegenden Berechnungen Bei Der Schwerkraftaufbereitung, *Z. Ver. deut. Ing.*, *77* (1933), pp. 318-326
[18] Johnson, *et al.*, Flow Past a Sphere up to a Reynolds Number of 300, *Journal of Fluid Mechanics*, 378 (1999), pp. 19-70

Paper submitted: March 10, 2017
Paper revised: May 1, 2017
Paper accepted: May 20, 2017